Vehicle sideslip angle estimation using Kalman filters: modelling and validation

PIERALICE, Cristiano, LENZO, Basilio <http://orcid.org/0000-0002-8520-7953>, BUCCHI, Francesco and GABICCINI, Marco

Vehicle Sideslip Angle Estimation Using Kalman Filters: Modelling and Validation

Cristiano Pieralice[1,2], Basilio Lenzo[2*], Francesco Bucchi[1], Marco Gabiccini[1]

[1] *Università di Pisa, Italy, e-mail: cpieralice@gmail.com, francesco.bucchi@unipi.it, marco.gabiccini@unipi.it*

[2] *Sheffield Hallam University,UK, e-mail: basilio.lenzo@shu.ac.uk*

Abstract. The knowledge of the vehicle sideslip angle provides useful information about the state of the vehicle and it is often considered to increase the performance of the car as well as to develop safety systems, especially in the vehicle equipped with Torque Vectoring control systems. This paper describes two methods, based on the use of Kalman filters, to estimate the vehicle sideslip angle and the tire forces of a vehicle starting from the longitudinal and yaw velocity data. In particular, these data refer to on-track testing of a Range Rover Evoque performing ramp steer maneuvers at constant speed. The results of the sideslip estimation method are compared with the actual vehicle sideslip measured by a Datron sensor and are also used to estimate the tire lateral forces.

Keywords: Sideslip angle, Kalman Filter, Vehicle, State estimation, Random walk method

1 Introduction

Over the last few decades, with the rapid development of assisted and automated driving, industrial and academic research has dedicated great effort towards safer and better performing vehicles. Nowadays, common cars are equipped with many active safety systems such as Anti-Lock Braking Systems (ABS) and Electronic Stability Control (ESC) systems. Each of them is based on control algorithms that take as inputs the data coming from inertial and velocity sensors that are commonly installed on vehicles. To date, to the best of the authors' knowledge, there is no commercial active system based on the direct measure of the sideslip angle. This parameter is more frequently used in more complex performance and safety systems, i.e. Torque Vectoring Systems [5,13,19], specifically using the vehicle sideslip angle in direct yaw moment controllers, to enhance vehicle safety [12,18]. The sideslip acquisition is obtained via two different ways: the first is a direct measurement by the use of expensive sensors which, most likely, cannot

equip commercial vehicles. The second strategy, more industrially appealing, is based on the estimation of the sideslip angle starting from the information provided by sensors (inertial and gyroscopic) commonly installed on commercial vehicles.

All the state of the art estimation methods in the literature can be classified as neural network-based or observer-based [4,7]. The former estimation method is based on training artificially intelligent systems where a database of input data (e.g. acceleration, wheel speed, steering wheel etc.) is provided to the estimator, along with the measured output (i.e. sideslip angle); the neural network adapts itself, without the use of a physical model, to minimize the error between the estimated and the measured output [1,11]. The latter category is based on a dynamic model of the system analysed, and can be subdivided further in two groups depending on the type of vehicle model adopted. In particular, observers have been proposed which are based either on kinematic models or on dynamic models [4]. Selmanaj et al. [17] present a kinematic-based model that uses a special parameter to define the mean longitudinal vehicle velocity. Chen et al. [3] also propose a kinematic model, along with an adaptive procedure to update the process noise covariance matrix at each time step. In [14] Madhusudhanan et al. estimate the lateral tire forces using a kinematic model and validate the results with measurements from special bearing sensors by SKF. In [8] Gadola et al. implement a dynamic model based on a single-track vehicle model. In [6,9,15] different authors propose dynamic models based on double-track vehicle models.

The present paper focuses on observer-based estimation, in particular on an Extended Kalman Filter (EKF) using a dynamic vehicle model. Two approaches are herein developed: the first is based on a Pacejka tire model, while the second is based on a random walk approach, which includes the tire lateral forces in the Kalman Filter state vector, and introduces a physical constraint to boost filter convergence. The two approaches have been tested on experimental data.

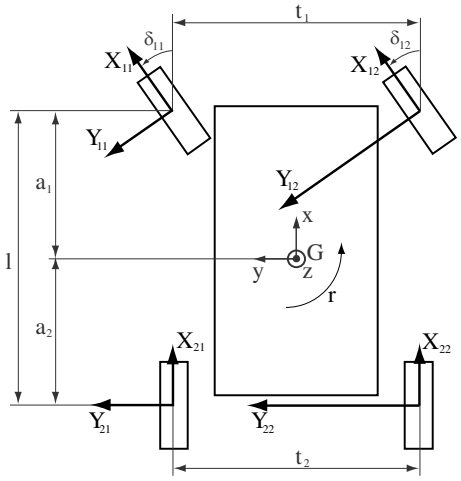

Fig. 1 Double-track vehicle schematic

2 Vehicle model

The vehicle model considered in this analysis is the two-track model shown in Fig. 1, where the main geometric and kinematic quantities are identified. The model includes some simplifying hypotheses, e.g. no geometric variations due to vehicle rolling and no effect on tire forces due to camber variation.

The system is described through three state variables: the longitudinal and lateral velocities, identified respectively with the letters u and v, and the yaw velocity, identified with r. The model equations are obtained from the translational equilibrium of the vehicle along the longitudinal (x) and lateral (y) axes, and from the rotational equilibrium equation around the z axis:

$$\begin{aligned}
\dot{u} &= \frac{1}{m}(X_{11}\cos\delta_{11} + X_{12}\cos\delta_{12} + X_{21} + X_{22} - Y_{11}\sin\delta_{11} - Y_{12}\sin\delta_{12} - F_D) \\
&\quad + vr \\
\dot{v} &= \frac{1}{m}(Y_{11}\cos\delta_{11} + Y_{12}\cos\delta_{12} + Y_{21} + Y_{22} + X_{11}\sin\delta_{11} + X_{12}\sin\delta_{12}) - ur \\
\dot{r} &= \frac{1}{J_z}((Y_{11}\cos\delta_{11} + Y_{12}\cos\delta_{12} + X_{11}\sin\delta_{11} + X_{12}\sin\delta_{12})a_1 - (Y_{21} + Y_{22})a_2 \\
&\quad + (X_{12}\cos\delta_{12} - X_{11}\cos\delta_{11})\frac{t_1}{2} + (X_{22} - X_{21})\frac{t_2}{2} + (Y_{11}\sin\delta_{11} - Y_{12}\sin\delta_{12})\frac{t_1}{2})
\end{aligned} \tag{1}$$

where m is the vehicle mass, J_z is the yaw moment of inertia, X_{ij} and Y_{ij} are respectively the longitudinal and lateral forces for each wheel ($j = 1$ left, $j = 2$ right) of each axle ($i = 1$ front, $i = 2$ rear), F_D is the drag force due to aerodynamics and rolling resistance, and δ_{1j} is the steering angle of each front wheel.

3 Kalman Filter theory and implementation

The KF, along with its variants, addresses the general problem of trying to estimate the state vector $\boldsymbol{x} \in \Re^n$ of a controlled process which, in the case of discrete time sampling, is governed by the generic set of equations [4]:

$$\begin{aligned}
\boldsymbol{x_k} &= f(\boldsymbol{x_{k-1}}, \boldsymbol{u_{k-1}}, \boldsymbol{w_{k-1}}) \\
\boldsymbol{z_k} &= h(\boldsymbol{x_k}, \boldsymbol{v_k})
\end{aligned} \tag{2}$$

where $\boldsymbol{u}$ is the system input, $\boldsymbol{z}$ the system output (i.e., the measured variables), $\boldsymbol{v}$ and $\boldsymbol{w}$, respectively, the process and measurement noise. The process noise models the inevitable difference between the dynamics of the actual system and the model used to represent it. On the other hand, $\boldsymbol{v}$ accounts for measurement errors**,** which depend, e.g., on the accuracy of the available sensors. The process noise and the measurement noise are assumed to have a Gaussian distribution with zero mean and covariance $\boldsymbol{Q}$ and $\boldsymbol{R}$, respectively for $\boldsymbol{w}$ and $\boldsymbol{v}$ [20]. In particular, the vehicle model is used in first instance, then the output is corrected based on the available measurements.

The Kalman Filter is grounded on the idea that the evolution of the state variables can be computed in a predictor-corrector fashion: i) the first step is the prediction of a future state through propagation forward in time of the current belief for state and covariance, according to Eq. (2); ii) the second step corrects the previous estimates in order to maximise the maximum a-posteriori probability to match the sensor readings. If the system is linear, Eq. (2) can be written as

$$\begin{aligned} \boldsymbol{x_k} &= A\boldsymbol{x_{k-1}} + F\boldsymbol{u_{k-1}} + \boldsymbol{w_{k-1}} \\ \boldsymbol{z_k} &= H\boldsymbol{x_k} + \boldsymbol{v_k} \end{aligned} \tag{3}$$

Denoting with $\widehat{\boldsymbol{x_k}}^-$ the state estimate at step k according to the dynamic evolution of the system (first equation in (2)), the KF estimation is

$$\widehat{\boldsymbol{x_k}} = \widehat{\boldsymbol{x_k}}^- + K_k(\boldsymbol{z_k} - H\widehat{\boldsymbol{x_k}}^-) \tag{4}$$

One form of K_k (denoted as Kalman gain) is given in [20] which depends on $\boldsymbol{Q}$ and $\boldsymbol{R}$. For example, if $\boldsymbol{Q}$ tends to zero, then $K \approx 0$ and $\widehat{\boldsymbol{x_k}} = \widehat{\boldsymbol{x_k}}^-$, which means that the model is deemed exceptionally accurate. On the other hand, if $\boldsymbol{R}$ approaches zero, i.e. in the hypothesis of an extremely reliable measurement, then $K \approx H^{-1}$ hence $\widehat{\boldsymbol{x_k}} \approx H^{-1}\boldsymbol{z_k}$, so the measurement is deemed representative of the state. Clearly neither of those limit conditions is satisfied in general: the Kalman Filter uses both the model and the measurements to estimate the state variables.

If the analyzed system is nonlinear (general form, Eq. (2)), it can be linearized and written in a form similar to Eq. (3), at the cost of some approximation. Such approach is known as Extended Kalman Filter (EKF) [20]. A different approach, denoted as Unscented Kalman Filter (UKF), is used for highly nonlinear system, generally performing better than the EKF but introducing significant complexities [4]. In this paper, an EKF is used, based on the vehicle model described in Section 2 and on the following measured signals:

- longitudinal velocity u, which is calculated as an average of the longitudinal component of each wheel center velocity, as described in [17];
- the yaw rate r, which is provided by the gyro sensor.

In a first implementation of the filter, the lateral forces Y_{ij} are calculated based on a Pacejka tire model [16]:

$$Y_{ij} = (A_1 Z_{ij} + A_2)\, Z_{ij} \sin(C \operatorname{atan} B\alpha_{ij}) \tag{5}$$

where coefficients A_1, A_2, B and C were available for the particular tire installed on the vehicle prototype, Z_{ij} are the vertical loads at each corner (computed taking into account static loads and load transfers), and α_{ij} are the tire slip angles of each vehicle corner. The tire slip angles α_{ij} were computed according to the well-known approach [2,10]:

$$\alpha_{ij} = \delta_{ij} - (\beta - (-1)^i \frac{r}{u} a_i) \tag{6}$$

where β is the sideslip angle. As well-known, a tire model such as Eq. (5) might not be actually representative of the real conditions, for instance due to tire wear, friction conditions, temperature etc. Therefore, in a further implementation of the

filter, a random walk approach was implemented (denoted in the remainder as EKF+RW). The idea is to add four variables in the state vector $\boldsymbol{x}$, i.e. the four lateral forces Y_{ij}, imposing their derivatives to be $\dot{Y}_{ij} = 0$ since no information on their dynamics was available. This means that the filter will also estimate Y_{ij}.

4 Model validation using experimental data

In order to validate the estimation methods, on-track acquired data have been considered. Such data were acquired on a vehicle equipped with four independent electric motors, one per wheel, and a Corrsys Datron S-350 sensor, measuring the vehicle sideslip angle (details on the whole experimental campaign are in [2]). In particular, two constant speed steering ramp maneuvers are considered, with reference constant speed 60 km/h and 80 km/h, and very low steering angle rate. Both the maneuvers were performed using a rear wheel drive (RWD) architecture with even torque distribution between left and right wheels. Here, the longitudinal forces X_{ij} were approximated as the ratio between each wheel torque (available for each drivetrain) and the wheel radius. To help the EKF+RW filter to converge, an additional measurement equation was implemented, imposing the overall vehicle yaw moment to be zero. Indeed due to the low steering angle rate, $\dot{r}$ (and thus the yaw moment, see Eq. (7)) is expected to be very small, as experimentally verified.

4.1 Sideslip angle estimation

Figure 2 shows the sideslip angle for the 60 km/h and 80 km/h maneuvers, obtained through the Datron direct measurements and through the estimation performed with the EKF and EKF+RW methods. For each maneuver the sideslip angle is initially zero (straight line trajectory before the steering pad) and it globally decreases as the lateral acceleration increases for both the measurement and the estimation results. The EKF+RW method shows better results than the EKF one, being the value of the estimated sideslip generally closer to the measured one, especially for high lateral accelerations. Concerning the EKF method, the results (in this section or in the following) are plotted only in the range of $a_y > 2$ m/s^2 for the 60 km/h maneuver and $a_y > 4$ m/s^2 for 80 km/h maneuver, because for lower acceleration values the estimated sideslip was extremely scattered. On the contrary, the sideslip angle values estimated via EKF+RW are significantly less scattered than those obtained through EKF and, especially for low values of lateral acceleration, no significant oscillation arises, being the estimated value correctly close to the real one even for almost straight-line trajectories. The accuracy of the results is fairly satisfactory because the error between the measured and EKF+RW estimated sideslip angle, detached from noisy signal oscillation, never exceeds ≈0.5 deg.

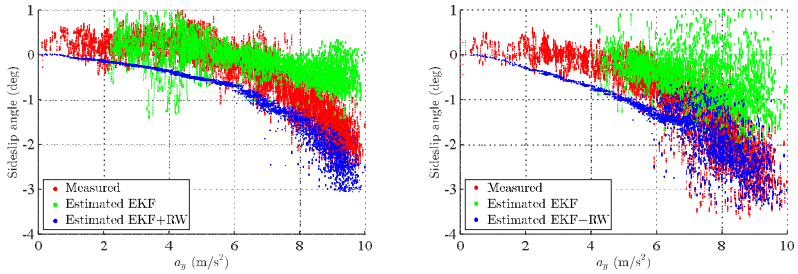

Fig. 2 Sideslip angle – 60 km/h (left) and 80 km/h (right) steering ramp

4.2 Lateral force and Yaw moment analysis

Since no direct measurement of each tire force was performed during the experimental campaign, the vehicle equilibrium was analyzed to validate the tire force estimation. In particular, the total lateral force Y and the yaw moment N were computed for both the real vehicle and the estimation models. Concerning the real vehicle, Y was obtained multiplying the acquired lateral acceleration by m, while N was obtained computing, after proper filtering, the time-derivative of the yaw velocity signal r multiplied by J_z. On the other hand, to compute Y and N in the models, it is necessary to know each (estimated) tire lateral force since, for the considered architecture, Y and N are defined as follows:

$$\begin{aligned} Y &= Y_{11}\cos\delta_{11} + Y_{12}\cos\delta_{12} + Y_{21} + Y_{22} \\ N &= ((Y_{11}\cos\delta_{11} + Y_{12}\cos\delta_{12})a_1 - (Y_{21} + Y_{22})a_2 + (Y_{11}\sin\delta_{11} \\ &\quad - Y_{12}\sin\delta_{12})\frac{t_1}{2} \end{aligned} \tag{7}$$

The total lateral force plots are shown in Fig. 3 for the 60 km/h and 80 km/h maneuvers. It is worth noting that the experimentally computed lateral force is, by definition, directly proportional to the lateral acceleration. The estimated total lateral force trend is satisfactory for the EKF+RW method, where both the data scattering and the error related to the experimentally computed total lateral force are restrained, particularly for the 60 km/h maneuvers. Higher data scattering appears at 80 km/h, which might also be ascrivable to the higher noise to signal ratio in the computation of δ_{11} and δ_{12} since, given the same lateral acceleration, the steering wheel angle is lower for the 80 km/h than for the 60 km/h maneuver. The data obtained through the EKF are more scattered and more distant from the experimentally computed values.

Similarly, the yaw moment plots are shown in Fig. 4 for the 60 km/h and 80 km/h maneuvers. The difference between the experimentally computed and the models estimated data is not negligible in this case, for both the EKF and the EKF+RW data. In particular, the EKF+RW method appears, here again, more ac-

curate than the EKF method, even if the data scattering (even for the experimentally computed data) is very high, especially for the 80 km/h maneuver.

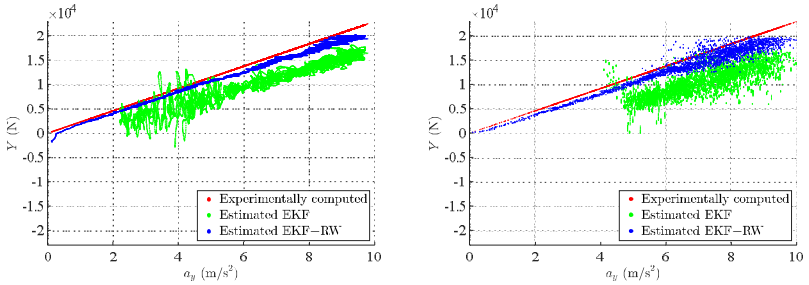

Fig. 3 Total lateral force – 60 km/h (left) and 80 km/h (right) steering ramp

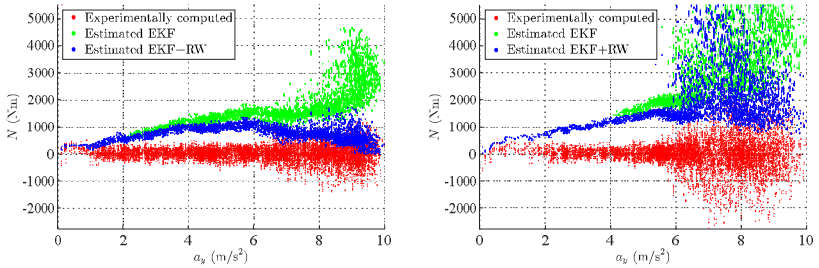

Fig. 4 Yaw moment – 60 km/h (left) and 80 km/h (right) steering ramp

5 Conclusions

In this paper two algorithms were presented which are grounded on Kalman Filter Theory and include also tire lateral forces as hidden states beside lateral, longitudinal and yaw velocities. In the first one, simply denoted as EKF, the lateral forces are linked to tire slips via the constitutive Pacejka equations, while in the second one, denoted as EKF+RW, the lateral forces are again treated as hidden states but obeying dynamics solely driven by noise (random walk model).

The validation of the two algorithms has been performed on the available direct measurements of the vehicle sideslip angle obtained by the accurate Datron sensor, showing satisfactory results, especially for the EKF+RW scheme, where the error never exceeds ≈ 0.5 degrees.

An indirect, additional assessment of the performance of the algorithms has been performed with the respect to their ability to reconstruct quantities not directly measurable, namely total lateral force Y and total moment N. Here, only the EKF+RW has shown the ability to output values comparable to physically plausible estimations on the basis of simple equilibrium considerations, while the EKF

has demostrated lower accuracy and a fairly high dispersion, especially for low acceleration values, in reconstructing the total force and total moment.

The simulation time of developed algorithms, implemented on a 2.26GHz CPU and 8 GB RAM laptop, was around 1/5 of the time of the actual maneuvers, thus endorsing a potential real time implementation.

As a future prospect, we envision further testing of the algorithms on transient-richer maneuvers, and there we expect the current force and torque reconstruction errors, to be become, despite the small steady-state error, much less significant.

References

1. Bucchi, F., Forte, P., Frendo, F.: Analysis of the torque characteristic of a magnetorheological clutch using neural networks. J. Intell. Material Syst. Struct, 26(6), 680-689 (2015)
2. Bucchi, F., et al.: The effect of the front-to-rear wheel torque distribution on vehicle handling: an experimental assessment. 25th Int. Symposium IAVSD 2017, Rockhampton, Australia (2017)
3. Chen, B.-C., Hsieh, F.-C.: Sideslip angle estimation using extended Kalman filter. Veh. Syst. Dyn. 46, 353–364 (2008)
4. Chindamo, D., Lenzo, B., Gadola, M.: On the Vehicle Sideslip Angle Estimation: A Literature Review of Methods, Models, and Innovations. Appl. Sci. 8, 355 (2018)
5. De Filippis, G. Lenzo, B., et al.: Energy-Efficient Torque-Vectoring Control of Electric Vehicles with Multiple Drivetrains, IEEE Transactions on Vehicular Technology, 67:6 (2018)
6. Doumiati, M., Victorino, A., Charara, A., Lechner, D.: A method to estimate the lateral tire force and the sideslip angle of a vehicle: Experimental validation. Proc. 2010 Am. Control Conf. (2010)
7. Farroni, F., et al.: A comparison among different methods to estimate vehicle sideslip angle. Proceedings of the World Congress on Engineering, Vol. 2 (2015)
8. Gadola, M., Chindamo, D., Romano, M., Padula, F.: Development and validation of a Kalman filter-based model for vehicle slip angle estimation. Veh. Syst. Dyn. 52, 68-84 (2014)
9. Ghosh, J., Tonoli, A., Amati, N., Chen, W.: Sideslip angle estimation of a Formula SAE racing vehicle. SAE Int. J. Passeng. Cars-Mechanical Syst. 9, 944–951 (2016)
10. Guiggiani, M., The Science of Vehicle Dynamics. Springer (2014)
11. Gurney, K., An introduction to neural networks. CRC press (2014)
12. Lenzo, B., Sorniotti, A., Gruber, P., Sannen, K.: On the experimental analysis of single input single output control of yaw rate and sideslip angle. Int. Journal of Automotive Technology, 18, 5 (2017)
13. Lenzo, B., De Filippis, G., et al.: Torque Distribution Strategies for Energy-Efficient Electric Vehicles with Multiple Drivetrains, ASME J. of Dyn. Systems, Meas. and Control, 139:12 (2017)
14. Madhusudhanan A.K., Corno, M., Holweg, E.: Vehicle sideslip estimator using load sensing bearings. Control Eng. Pract. 54 (2016)
15. Ouahi, M., Stéphant, J., Meizel, D.: Simultaneous observation of the wheels' torques and the vehicle dynamic state. Veh. Syst. Dyn. 51, 737-766 (2013)
16. Pacejka, H.B.: Tire and Vehicle Dynamics (2006)
17. Selmanaj, D. Corno, M., Panzani, G., Savaresi, S.M.: Vehicle sideslip estimation: A kinematicbased approach. Control Eng. Pract. 67 1–12 (2017)
18. Tota, A., et al.: On the experimental analysis of integral sliding modes for yaw rate and sideslip control of an electric vehicle with multiple motors. Int. Journal of Automotive Technology (2018)
19. Wang, Z., Montanaro, U., Fallah, S. et. al.: A gain scheduled robust linear quadratic regulator for vehicle direct yaw moment control. Mechatronics, 51, pp.31-45 (2018)
20. Welch, G., Bishop, G.: An Introduction to the Kalman filter. University of North Carolina at Chapel Hill, Department of Computer Science, TR 95-041 (2004)